REAL-TIME RFI EXCISION FOR THE GMRT WIDEBAND CORRELATOR

Kaushal D. Buch, Yashwant Gupta, Shruti Bhatporia, Swapnil Nalawade, Kishor Naik, Ajithkumar B.

Giant Metrewave Radio Telescope, NCRA-TIFR
Digital Backend Group,
Pune, Maharashtra, 410504, India

ABSTRACT

Real-time RFI excision is developed for the GMRT wideband correlator as part of the upgraded GMRT (uGMRT) project. The technique uses robust statistical estimation and a non-linear filter to excise broadband and narrowband RFI. This paper provides an overview of the technique and its real-time implementation. The results showing improvement in the signal-to-noise ratio and cross-correlation performance are also provided.

***Index Terms*— RFI, Median Absolute Deviation, GMRT, Radio Telescope, Correlator**

1. INTRODUCTION

The Giant Metrewave Radio Telescope (GMRT)[1] is an antenna array for observing astrophysical phenomena at radio frequencies ranging from 150 MHz to 1450 MHz. It is a passive radiometer which measures total and correlated power from an astronomical source. GMRT is undergoing an upgrade which will lead to an improvement in the sensitivity, primarily through increased receiver bandwidth. With a wider bandwidth, the GMRT is also likely to encounter higher levels of RFI. A real-time RFI mitigation technique is being developed to achieve the desired sensitivity in presence of RFI. This real-time technique detects and filters RFI and is implemented in the GMRT wideband digital backend (GWB) [2].

A large fraction of the RFI at the GMRT is impulsive in time or frequency domain. Based on its spectral spread, the RFI impulsive in time domain is called broadband RFI, and that which is impulsive in the frequency domain is called narrowband RFI. Impulsive RFI causes the Gaussian distribution of the signal in time domain to become heavy-tailed. The RFI mitigation scheme chosen (in both domains) is an impulse removal technique which belongs to a class of RFI mitigation methods called Excision [3, 4]. Median Absolute Deviation (MAD) is chosen as a robust estimator for computing filtering threshold and RFI detection. The detected sample can be replaced by a constant value or noise. Real-time excision is implemented at different locations in the GWB correlator chain as shown in Fig. 1. The real-time implementation is carried out on FPGA and CPU-GPU platforms. This paper provides an overview of the real-time RFI excision system for the uGMRT along with the results and current developments. The paper also proposes techniques for estimating MAD for strong and persistent RFI. Tests carried out show 10 dB improvement in the signal-to-noise ratio and in the cross-correlation properties of the signal.

2. REAL-TIME RFI EXCISION

Real-time RFI excision in the GWB is carried out by robust thresholding of the signal followed by non-linear filtering. Median and MAD are used as robust estimators for the location and dispersion of the signal. Robust estimators provided an unbiased statistical estimate in the presence of outliers (RFI). Median and MAD provide unbiased estimate up to 50% samples (breakdown point) corrupted by RFI in a window. In order to get the robust standard deviation, MAD is scaled by a factor of 1.4826 when the underlying distribution is Gaussian. [5]. For a input data vector X, the upper and lower thresholds, τ_U and τ_L respectively, are calculated using the sample median $M(X)$ and the robust standard deviation (σ_R) as

$$\begin{aligned} \tau_U &= M(X) + n \times (1.4826 \times \sigma_R) \\ \tau_L &= M(X) - n \times (1.4826 \times \sigma_R), \end{aligned} \tag{1}$$

where, n is the multiplying factor for the upper and lower thresholds. The input signal is compared with the robust thresholds and value outside the thresholds is replaced by a constant value or noise sample. The noise sample has statistics similar to the input signal.

2.1. Median of MAD values

The window size for estimating median and MAD depends on the duration of RFI and sampling period of the signal. Also, not more than 50% of the samples must be corrupted by RFI for an unbiased estimation. The longer the duration of RFI, the larger is the window size required for an unbiased estimation. MAD computation for a large window size is a challenge due to practical limitations arising from resource constraints.

978-1-5090-6201-0/16/$31.00 ©2016 IEEE

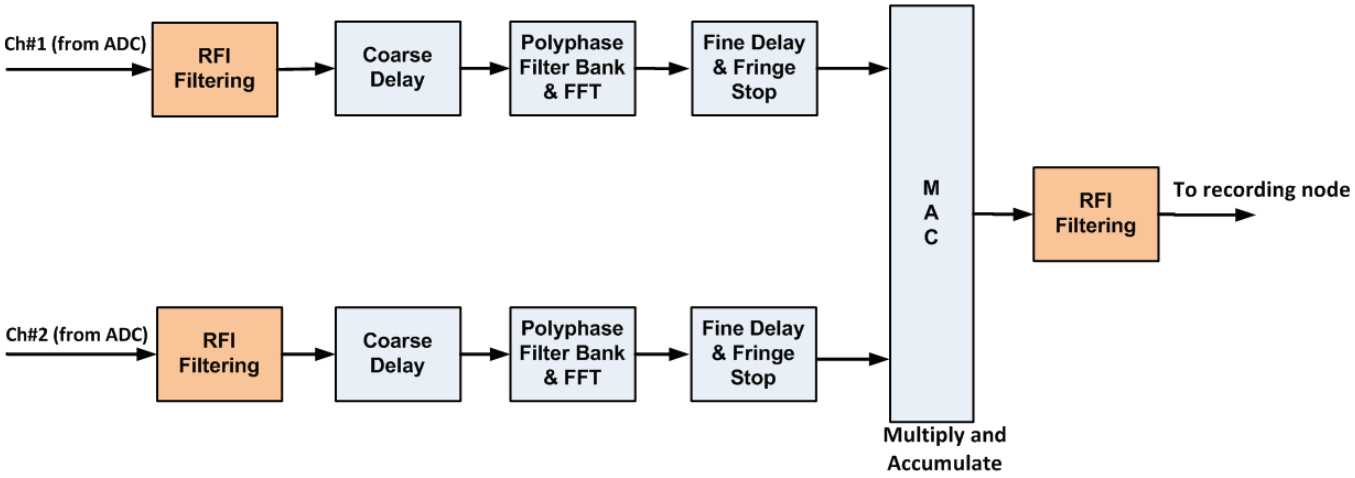

Fig. 1. Block Diagram of the GMRT wideband correlator along with the real-time RFI excision blocks

A technique proposed here helps in getting an unbiased estimate even in presence of persistent RFI and smaller window size. MAD values calculated from successive windows, smaller in size, are stored in memory. The median of several stored MAD values is carried out to get an estimate of MAD in presence of persistent RFI. For K MAD values computed on smaller window sizes, the median (M) of MAD values M_K is

$$M_K = M(MAD_1, MAD_2, ..., MAD_K). \quad (2)$$

2.2. Quantitative Metric

The performance of RFI filtering is quantified by a ratio of mean to the root mean square (RMS) value of the signal. This ratio is a normalized quantity and is robust to system gain fluctuations in the RF and analog receiver subsystems. The mean-to-RMS ratio (μ/σ) for a radio telescope receiver is given as $\sqrt{B \times T}$, where μ, σ, B, T are the sample mean, sample RMS, bandwidth and integration time of the system respectively. The mean-to-RMS ratio will reach its theoretical limit given by $\sqrt{B \times T}$ for a Gaussian distributed random signal. Generally, for a Gaussian distributed signal corrupted by impulsive RFI, the mean-to-RMS ratio will get affected since the signal distribution becomes heavy-tailed.

The improvement metric (I) in dB derived from the mean-to-RMS ratio is

$$I = 10log(MR_F/MR_U)\ \ dB, \quad (3)$$

where MR_U and MR_F are the mean-to-RMS ratio for the unfiltered and filtered signal respectively.

3. REAL-TIME BROADBAND RFI EXCISION

Broadband RFI filtering using MAD is carried out on GWB for 60 inputs (30 antennas, dual polarization) each having 400 MHz bandwidth. To process Nyquist-sampled time-series for 8-bit precision, the parallelism in the FPGA was utilized. It was found that the computationally intensive operation, MAD, is suitable for real-time implementation using the histogram method. Using the histogram method to calculate median and MAD, the real-time and resource requirements were met for Xilinx Virtex-5 SX95T FPGA available on ROACH-1 board (https://casper.berkeley.edu/wiki/ROACH). The design is available as part of the CASPER open-source library (https://casper.berkeley.edu/wiki/Projects)

3.1. Results from antenna and emulator tests

Real-time broadband RFI filtering is tested for the beamformer and correlator modes of the GWB at integration time of 1.3 ms and 671 ms respectively. Since broadband RFI affects all the spectral channels equally, the analysis is carried out on a single spectral channel output for a pair of antennas. Three copies of each signal are created in order to get a simultaneous comparative analysis of the two filtered and one unfiltered output. Detection and filtering are carried out at 800 MHz on consecutive windows, each containing 4096 data samples with 8-bit data precision. GWB outputs from a short baseline (two antennas) of GMRT are recorded simultaneously in the beamformer mode and the correlator mode. A short baseline is chosen to get correlated RFI signals. The signals from both the antennas are processed with and without RFI filtering to understand the effect on cross-correlation.

The temporal behavior of a single spectral channel with unfiltered and filtered data corresponding to 636 MHz radio frequency is shown in Fig. 2. In this experimental setup, two antennas, say, A1 and A2 are connected to the input of the GWB system and observe the astronomical source 3C48. The results show a comparative analysis between unfiltered and filtered data processed simultaneously through the GWB. The first subplot is the beamformer mode intensity data for

978-1-5090-6201-0/16/$31.00 ©2016 IEEE

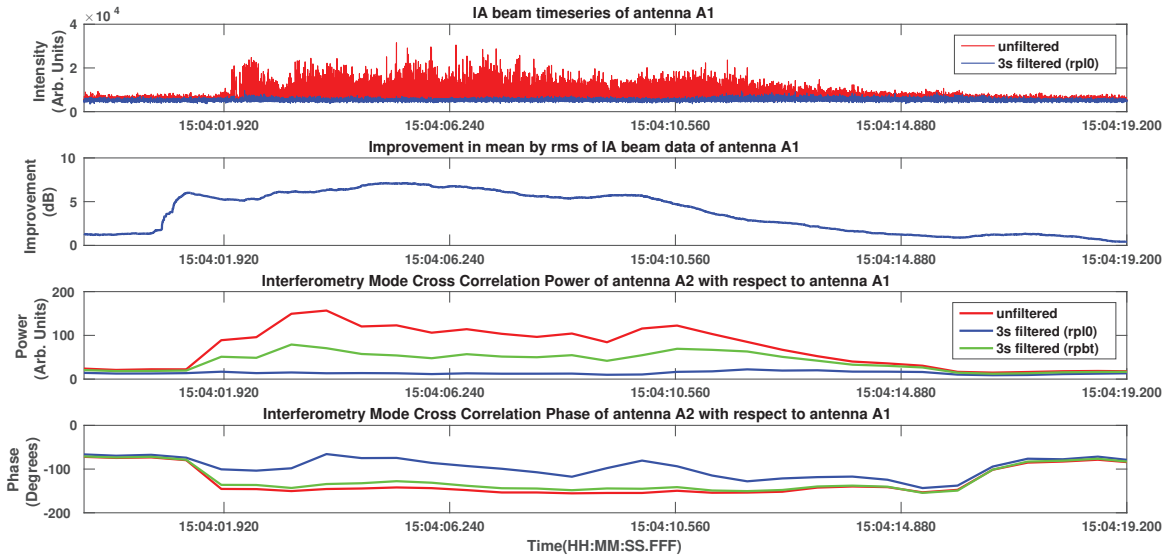

Fig. 2. Broadband RFI filtering for antenna signals in correlator and beamformer modes

filtered (shown in blue) and unfiltered (shown in red) options. The X-axis shows the time at which the data was recorded. RFI is filtered at 3σ threshold in time-domain and the detected samples are replaced by $zero$. The second subplot shows improvement in the mean-to-RMS ratio which is calculated as shown in section 2.2 over 1024 samples of the beamformer data. A maximum of 7 dB improvement is observed in this case.

The third and fourth subplots are time aligned with the first subplot and show amplitude and phase of the cross-correlation for antenna A2 with respect to antenna A1. Two different filtering options, replacement by $zero$ (shown in blue) and replacement by $threshold$ (shown in green) are compared with the unfiltered signal (shown in red) in the third and fourth subplots. Generally, for short baselines, the cross-correlation amplitude increases in the event of correlated RFI (shown in red). RFI Filtering reduces the amplitude of the cross-correlation towards its desired values. The phase of the cross-correlation fluctuates in the event of RFI as seen in the fourth subplot. Under normal conditions, the phase for a point source should not have large fluctuations especially when observed for a short duration. The phase of the filtered signal is maintained at the same value as it was in the absence of RFI. The effect of replacement with $zero$ (shown in blue) and $threshold$ (shown in green) value are overlayed in the third and fourth subplots. In this case, replacement with $zero$ provides better performance over replacement by $threshold$.

3.1.1. Tests using RFI emulator

RFI emulator is an analog instrument developed at the GMRT to generate RFI with desired duration and power in order to test the filtering system under controlled conditions. It generates a broadband noise floor and adds periodic broadband RFI signal or pulsed noise with a specific duty cycle and having average power greater than the noise floor. The duty cycle is programmable. The output from the emulator can be fed as baseband signal to the GWB system. For the example shown in Fig. 3, the on period of the RFI is $16\mu s$ and $total$ period is $2s$. The tests have been carried out with the GWB and RFI filtering configuration similar to those for the antenna signals described earlier in this section. Fig. 3 shows the effect of filtering observed at 1.3 ms time resolution beamformer output for an input signal generated using the emulator. As can be seen in the first subplot, the unfiltered time-series shows periodic occurrences of RFI (pulsed-noise) which are filtered out at 3σ threshold and replaced by $zero$. The corresponding improvement (in dB) is shown in the second subplot. Improvement is calculated over 1024 of the beamformer data shown in subplot 1.

4. NARROWBAND RFI EXCISION

The detection of narrowband RFI is done in the post-FFT section after temporal integration (Ref. Fig. 1) using MAD based estimation (of dispersion) across the spectrum. Based on the trade-off between the relative strength of the narrowband RFI as compared to the total receiver noise, the detection can be carried at different levels of temporal integration. It is possible to detect narrowband RFI buried in the system noise after temporal integration of consecutive spectra. The power variation across the spectrum due to receiver characteristics can influence the MAD estimation and can lead to sub-optimal

978-1-5090-6201-0/16/$31.00 ©2016 IEEE

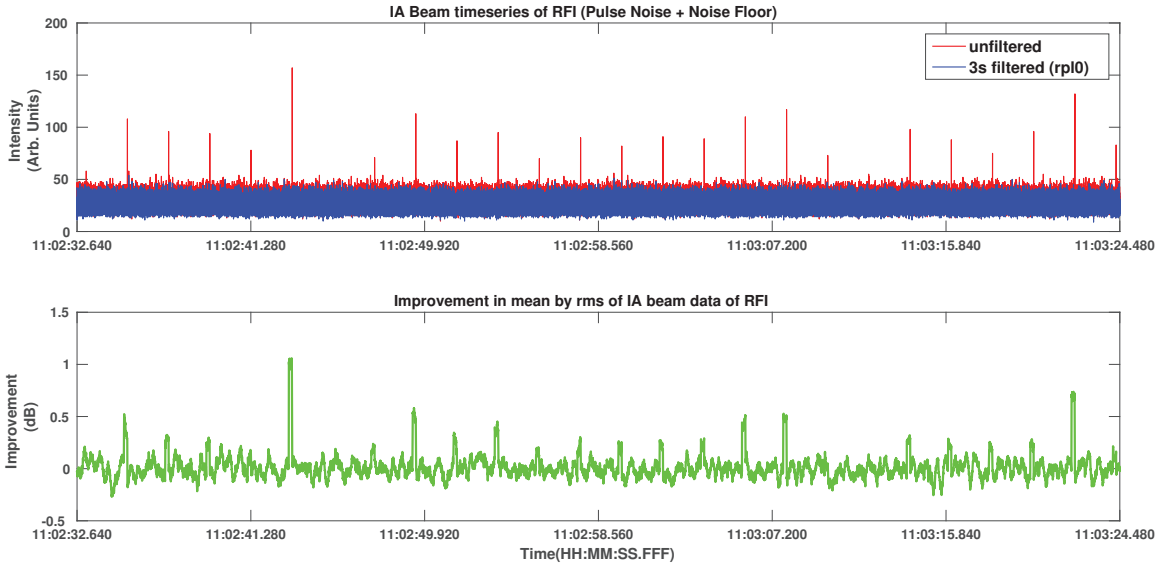

Fig. 3. Broadband RFI filtering for emulator signal in high time-resolution (beamformer) mode

filtering. Thus, a spectral normalization has to be carried out before the filtering operation.

4.1. Results on recorded GWB data

Narrowband RFI filtering at 3σ threshold is carried out on data recorded at 671 ms time resolution from the GMRT correlator in the 500 - 700 MHz band. There are several narrowband RFI lines as seen in subplot 1 of Fig. 4. MAD-based filtering shows improvement after spectral normalization and replacement of channels having RFI with $threshold$ as seen in subplot 2. The channels that are flagged are shown by the 'flagged data' plot between the two subplots.

4.2. Towards real-time implementation on GWB

The narrowband RFI filtering described earlier works on recorded correlator data. Development is underway to implement this feature in real-time on temporally integrated correlator output. In the GWB system, the integrated data from the compute engines (CE) forming the GPU cluster is sent to the recording node through a network switch (Fig. 5). This node receives the correlator data for all the antennas. The base integration period at which the data is integrated in the GPU cluster is 671 ms. Narrowband RFI filteirng on correlation spectra would be implemented at this point. The algorithm implementation would be carried out on the CPU of the recording node. For this purpose, the data would be read from the shared memory of the recording node machine and buffered prior to the real-time filtering operation. Narrowband RFI filter would generate filtered data and flags corresponding to spectral channels containing RFI. The filtered output may be temporally integrated before being recorded on hard disk.

5. CONCLUSION

MAD-based real-time RFI excision techniques developed for the GMRT wideband correlator were described along with their real-time implementation and test results. Tests were carried out to evaluate the performance of different RFI filtering options by using signals from antenna and RFI emulator. The results show improvement in the signal-to-noise ratio and cross-correlation performance. Real-time RFI excision is now available as a feature in the GMRT wideband correlator. These techniques can be used in the existing and upcoming radio telescopes like the Square Kilometer Array (SKA) and also in microwave radiometers for remote sensing.

6. ACKNOWLEDGMENT

The authors would like to thank Sanjay Kudale for his help in data analysis. The authors would also like the members of the backend group and control room at GMRT.

7. REFERENCES

[1] Govind Swarup, S Ananthakrishnan, VK Kapahi, AP Rao, CR Subrahmanya, and VK Kulkarni, "The Giant Metrewave Radio Telescope," 1991.

[2] B Ajithkumar, SC Choudhari, KD Buch, MV Muley, GJ Shelton, SH Reddy, S Kudale, J Roy, and Y Gupta,

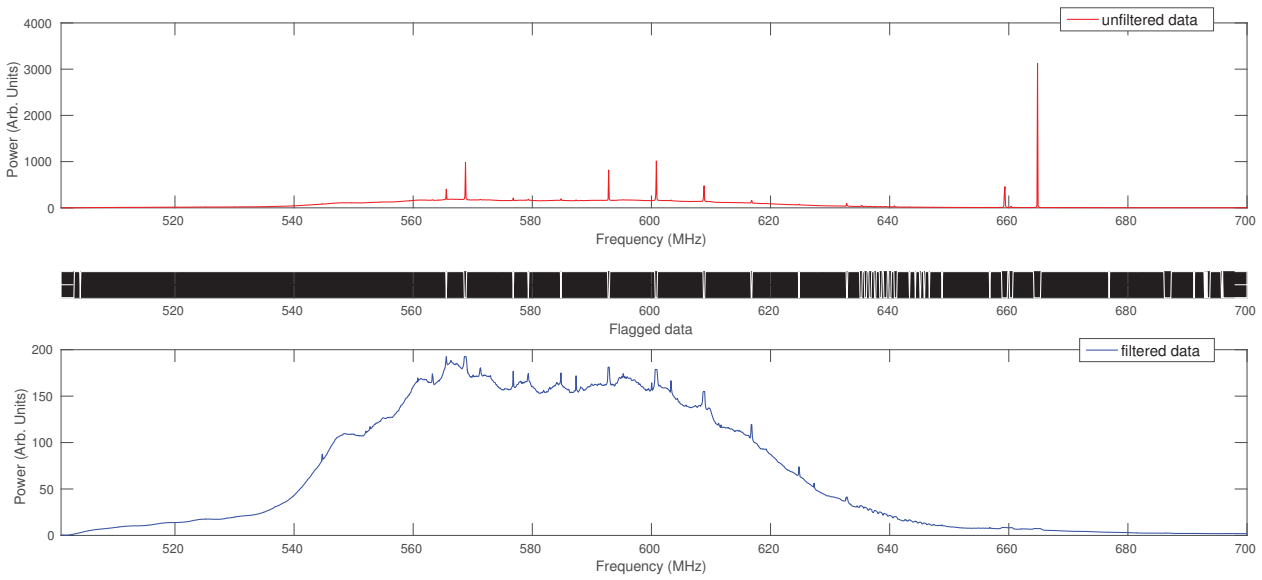

Fig. 4. Narrowband RFI filtering at 3σ threshold

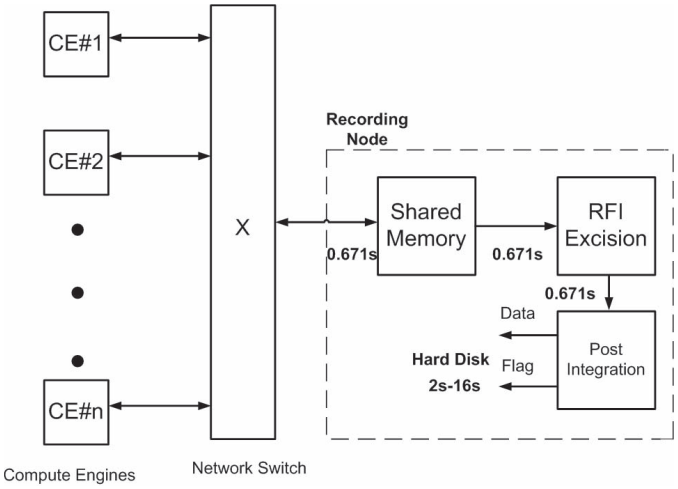

Fig. 5. Proposed scheme for implementation of real-time narrowband RFI filtering

"Next generation digital backends for the GMRT," in *IOP Conference Series: Materials Science and Engineering*. IOP Publishing, 2013, vol. 44, p. 012024.

[3] RA Series, "Techniques for mitigation of radio frequency interference in radio astronomy," 2013.

[4] PA Fridman, "Statistically stable estimates of variance in radio-astronomy observations as tools for radio-frequency interference mitigation," *The Astronomical Journal*, vol. 135, no. 5, pp. 1810, 2008.

[5] Peter J Rousseeuw and Christophe Croux, "Alternatives to the median absolute deviation," *Journal of the American Statistical association*, vol. 88, no. 424, pp. 1273–1283, 1993.

978-1-5090-6201-0/16/$31.00 ©2016 IEEE